Plectin-controlled keratin cytoarchitecture affects MAP kinases involved in cellular stress response and migration

Selma Osmanagic-Myers, Martin Gregor, Gernot Walko, Gerald Burgstaller, Siegfried Reipert, and Gerhard Wiche

Department of Molecular Cell Biology, Max F. Perutz Laboratories, University of Vienna, A-1030 Vienna, Austria

Plectin is a major intermediate filament (IF)–based cytolinker protein that stabilizes cells and tissues mechanically, regulates actin filament dynamics, and serves as a scaffolding platform for signaling molecules. In this study, we show that plectin deficiency is a cause of aberrant keratin cytoskeleton organization caused by a lack of orthogonal IF cross-linking. Keratin networks in plectin-deficient cells were more susceptible to osmotic shock–induced retraction from peripheral areas, and their okadaic acid–induced disruption (paralleled by stress-activated MAP kinase p38 activation) proceeded faster. Basal activities of the MAP kinase Erk1/2 and of the membrane-associated upstream protein kinases c-Src and PKCδ were significantly elevated, and increased migration rates, as assessed by in vitro wound-closure assays and time-lapse microscopy, were observed. Forced expression of RACK1, which is the plectin-binding receptor protein for activated PKCδ, in wild-type keratinocytes elevated their migration potential close to that of plectin-null cells. These data establish a link between cytolinker-controlled cytoarchitecture/scaffolding functions of keratin IFs and specific MAP kinase cascades mediating distinct cellular responses.

Introduction

Plectin is an intermediate filament (IF)–associated cytolinker protein of very large size ($M_r > 500,000$) and with versatile functions (for review see Wiche, 1998). It is expressed in a wide variety of mammalian cells and tissues and has important functions in mediating interactions between different cytoskeletal network systems and their anchorage at cell–cell and cell–matrix junctional complexes. Plectin's IF-binding site was mapped to a stretch of ∼50 amino acid residues linking two (5 and 6) of its six C-terminal repeat domains. At its N terminus, plectin harbors a functional actin-binding domain that also serves as an integrin β4- and an additional vimentin-binding site (Sevcik et al., 2004). Plectin's association with microtubules and their cross-linking to vimentin IFs has been previously reported (Svitkina et al., 1996); however, the molecular mechanism of this interaction is still unknown.

There is increasing evidence that, apart from acting as a cytoskeletal linker protein, plectin serves an important function as a scaffolding platform of proteins involved in cellular signaling. Strong support for this idea comes from the recent identification of several novel interaction partners of plectin with links to signaling, such as the nonreceptor tyrosine kinase Fer and AMP kinase, and the observation that plectin deficiency affects their enzymatic activities (Lunter and Wiche, 2002; Gregor et al., 2006). The scaffolding function of plectin was recently confirmed when it was shown that the protein binds and sequesters the receptor for activated C kinase 1 (RACK1) to the cytoskeleton, and thereby affects PKC signaling pathways (Osmanagic-Myers and Wiche, 2004). This, together with previous studies showing that plectin is involved in the regulation of actin filament dynamics and influences Rho/Rac/cdc42 signaling (Andrä et al., 1998), suggests that plectin, and likely cytolinkers in general, provide a crucial link between cytoskeleton dynamics and signaling machineries.

The prominent localization of plectin at hemidesmosomes (HDs), desmosomes, Z-line structures and dense plaques of striated and smooth muscle, intercalated discs of cardiac muscle, and focal contacts implied a role for the protein in linking the cytoskeleton to plasma membrane junctional complexes (Wiche, 1998). This was supported by studies showing that defects in plectin expression lead to the skin disease epidermolysis bullosa simplex (EBS). In these patients, as well as in plectin-deficient

mice generated by targeted gene inactivation (Andrä et al., 1997), the link of the keratin cytoskeleton to HDs was dramatically affected (McMillan et al., 1998), with keratin filaments appearing less tightly bundled at their insertion into the inner plate structure of HDs. Moreover, earlier ultrastructural studies and in vitro reconstitution of IFs had shown that plectin was primarily located at branching points of IFs (Foisner et al., 1988). However, the important question of whether plectin, indeed, affects IF network cytoarchitecture and its dynamics has not been addressed so far, except for a study showing that a recombinant fragment containing plectin's C-terminal IF-binding site inhibits IF formation in vitro in a dose-dependent manner (Steinböck et al., 2000). Investigating what impact plectin deficiency has on the organization and dynamic properties of IFs in keratinocytes, we found a direct link between plectin-controlled IF cytoarchitecture and MAP kinase signaling cascades involved in cell migration and stress response.

Results

Plectin, a major organizing element of IF cytoarchitecture in keratinocytes

To investigate whether plectin plays a role in IF network organization, we first compared the general appearance of such networks in plectin wild-type (ple [+/+]) and plectin-deficient (ple [−/−]) basal keratinocytes using immunofluorescence microscopy. In interior cytoplasmic regions, both primary and p53-deficient ple (+/+) keratinocytes exhibited dense networks of keratin filaments. The filaments showed partial colocalization with discontinuous plectin-positive structures, which in superimposed images often resembled beads on a string (Fig. 1, A and G). However, at the cell margins, hardly any IFs were found, leaving a peripheral ring–shaped, filament-free zone densely packed with plectin structures. Keratin filaments extended to the inner circumference of this ring (Fig. 1, A and G, arrows), as if peripheral plectin acted in an inhibitory manner on filament extension. In support of this view, the keratin network system of wild-type cells seemed to be more densely packed around the cell center compared with that of ple (−/−) cells, where it extended further to the cell periphery (Fig. 1, compare B and H with E and K, respectively). This phenotype was noticed independent of whether the anti-pan keratins K5, K6, and K18 or anti-K5 or K6 antibodies alone were used (Fig. 1; unpublished data). Furthermore, particularly in subconfluent cell cultures (∼60% confluence), ple (−/−) cells exhibited significantly enlarged mesh size of keratin networks at their periphery compared with wild-type cells (Fig. 1, compare B with E and H with K, along with their corresponding magnifications). A quantitative analysis of subconfluent cell populations revealed that >70% of ple (−/−), but only <8% of ple (+/+), keratinocytes displayed such a phenotype. Regarding expression levels of different keratins, no differences were observed between ple (+/+) and (−/−) keratinocytes, as revealed by immunoblotting analysis (Fig. S1, available at http://www.jcb.org/cgi/content/full/jcb.200605172/DC1). Interestingly, the vimentin filament network of plectin-deficient fibroblasts showed similar characteristics. It appeared more bundled and less delicate compared with
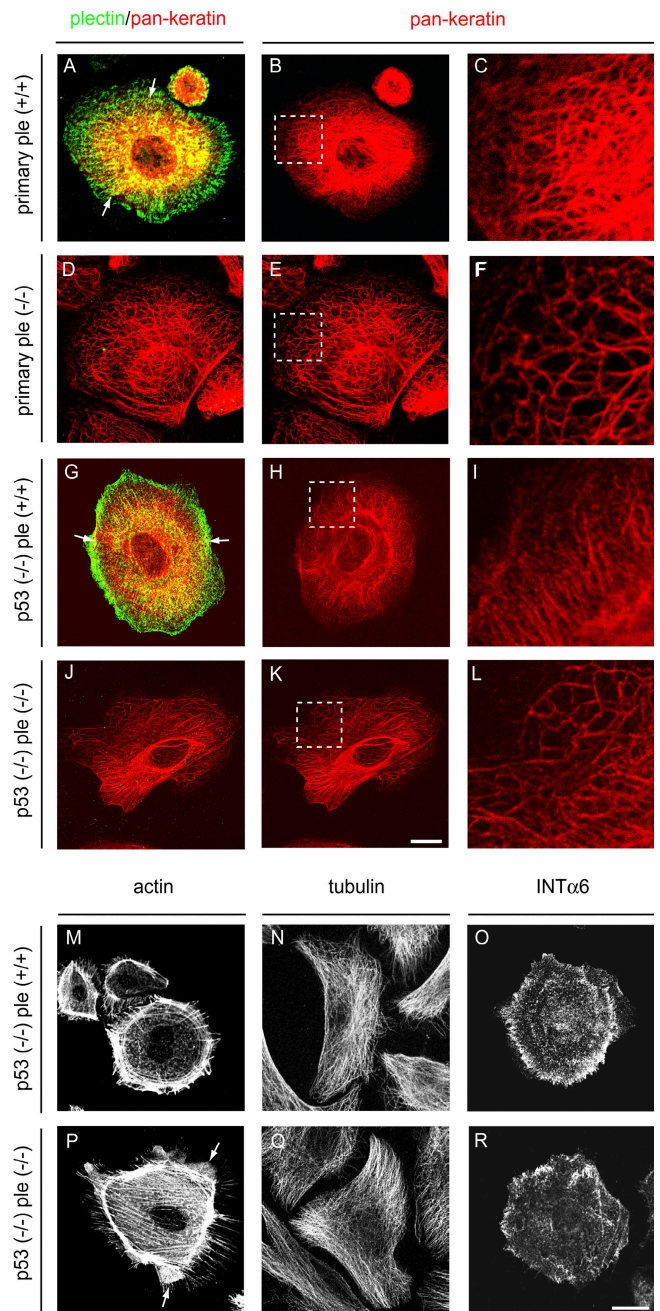

Figure 1. **Cytoarchitecture of keratin filament networks in wild-type and plectin-deficient basal mouse keratinocytes.** Cells were double immunolabeled using antiserum to plectin and mAbs to pan-keratin (A–L), or single-labeled as indicated (M–R). Boxed areas in B, E, H, and K are shown as 4×-magnified images in (C, F, I, and L), respectively. Arrows in A and G, peripheral endings of keratin filaments. Arrows in P, newly formed lamellipodia. Bars in K and R (representative of A, B, D, E, G, H, J, K, and M–R, respectively), 10 μm.

wild-type cells, creating a network with wider spaces between the filaments (unpublished data).

In both ple (+/+) and (−/−) cells, actin filaments exhibited a subcortical organization typical of subconfluent keratinocyte cultures (Fig. 1, M and P; Vasioukhin et al., 2000). However, ple (−/−) keratinocytes showed a slight increase in the number of stress fibers and, moreover, were extending small lamellipodia (Fig. 1 P, arrows), which is indicative of an ongoing transition
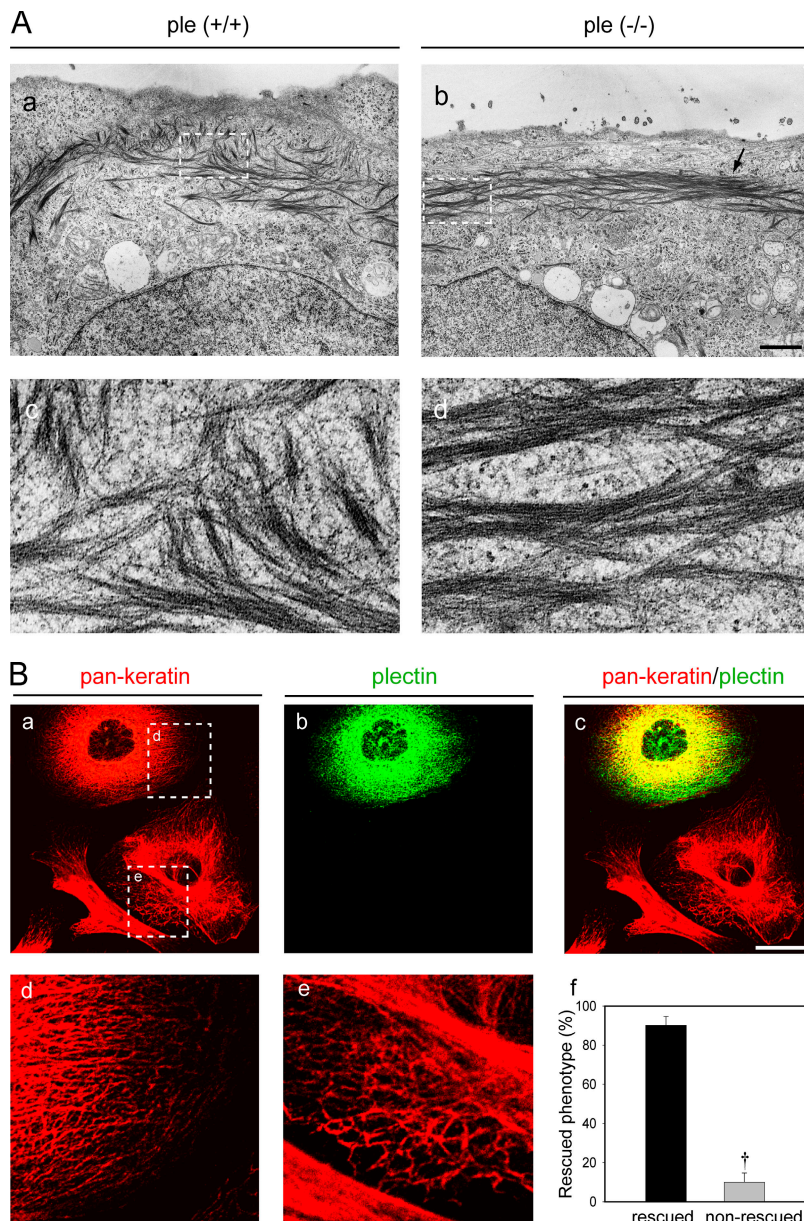
Figure 2. **Plectin reduces the mesh size of IF networks.** (A) Keratinocytes were subjected to transmission electron microscopy, as described in the text. Boxed areas in a and b are shown as 7×-magnified images in c and d, respectively. Arrow in b marks massively bundled keratin filaments. (B, a–e) ple (−/−) keratinocytes transfected with full-length plectin (isoform 1a) were fixed and immunolabeled for pan-keratin and plectin. Boxed areas in a are shown as 4×-magnified images in d and e. Note that there are more delicate filamentous network in cells upon forced expression of plectin (d). (f) Rescue efficiency was determined by analysis of >100 ple (−/−) cells transiently expressing plectin (three independent experiments). Keratinocytes with average filament–filament distances of below or above 1.5 nm were considered as rescued and non-rescued, respectively. Mean values ± the SEM are shown. †, $P < 0.001$. Bars: (A) 1 μm; (B) 10 μm.

from a stationary to a migratory phenotype. Furthermore, no gross differences were observed between ple (+/+) and (−/−) cells in the organization of microtubules (Fig. 1, N and Q). Peripheral integrin (INT) α6 clusters were formed in both cell types (Fig. 1, O and R), and in ple (+/+) cells, partial colocalization with plectin was observed (Fig. S2, A–C, available at http://www.jcb.org/cgi/content/full/jcb.200605172/DC1). In addition, keratin staining partially overlapped with the ring formed by integrin clusters (Fig. S2, D–F).

Transmission electron microscopy revealed a prominent lateral bundling of keratin filaments in peripheral regions of ple (−/−) cells, resulting in larger spaces between individual and bundled filaments (Fig. 2 A, b and d). In some regions, filaments showed a complete lateral collapse, appearing as one massive filamentous bundle (Fig. 2 A, b, arrow). Bundling to such an extent was never observed in ple (+/+) cells, where corresponding areas were dominated by numerous fine, and apparently short, filamentous structures, with orthogonal cross-bridges filling the space between the filament bundles (Fig. 2 A, a and c).

To demonstrate that the observed changes in keratin network organization were directly connected to plectin deficiency, the phenotypic rescue potential of plectin was examined by transient transfection of ple (−/−) keratinocytes with an expression plasmid encoding full-length mouse plectin isoform 1a, which is the major isoform normally expressed in this type of cells (Andrä et al., 2003). Similar to endogenous plectin of corresponding wild-type cells (Fig. 1 G), reexpressed plectin 1a showed a punctated distribution pattern (Fig. 2 B, b). A quantitative analysis revealed that 90% of ple (−/−) cells expressing plectin 1a at significantly high levels displayed keratin networks with mesh sizes as small as those of ple (+/+) cells (Fig. 2 B, f). This strong rescue potential of plectin 1a clearly demonstrated a direct link between the absence of plectin and the observed alterations of the keratin network cytoarchitecture.

Keratin filaments of ple (−/−) keratinocytes are more sensitive to hypoosmotic shock

Osmotic and heat-shock assays serve as useful tools in monitoring keratin network properties and their alterations in EBS caused by keratin mutations (Morley et al., 1995; D'Alessandro et al., 2002). Therefore, we examined whether the altered keratin filament cytoarchitecture of ple (−/−) keratinocytes affected their response to changes in osmolarity and temperature. Upon urea treatment, INTα6-positive retraction fibers, which are a characteristic feature of migrating and mitotic cells (Geuijen and Sonnenberg, 2002), became very pronounced at the rear of both cell types (Fig. 3 A, a, c, d, f, h, and i). Most probably, the general shrinkage of the cells, which started shortly after exposure to urea (D'Alessandro et al., 2002), triggered the elevated formation of these structures. INTα6-positive retraction fibers of ple (−/−) cells, however, were significantly longer than those of ple (+/+) cells, possibly reflecting a stronger shrinkage of plectin-deficient cells (Fig. 3 A, compare d and i). In accordance with recent studies showing increased urea-induced bundling of keratin filaments (Werner et al., 2004), the IF network appeared less filamentous after urea treatment and accumulated around the cell center, indicating that it had collapsed onto the nuclei (Fig. 3 A, b and g). Interestingly, at the leading edge of cells, which is an area devoid of retraction fibers, keratin bundles of ple (+/+) cells displayed a regular form and were closely associated with peripheral integrin clusters, whereas in ple (−/−) cells filament bundles were conspicuously tangled and distant from the cell periphery (Fig. 3 A, compare e and j). The appearance of such "torn" filaments in ple (−/−) cells suggested a reduction in their INTα6β4 anchorage. This would be consistent with the reduced attachment of keratin filaments to HDs reported for EBS patients (McMillan et al., 1998).

To address this issue biochemically, we prepared cytokeratin-enriched cell fractions from ple (+/+) and (−/−) keratinocytes grown on collagen I and compared their INTα6β4 content using antibodies to INTβ4. As expected, such cell fractions were highly enriched in keratins 5 (unpublished data) and 14 (Fig. 3 B) and,

in the case of wild-type cells, contained considerable amounts of plectin. INTβ4 was, however, completely absent from cytokeratin fractions of ple (−/−) cells. The absence of INTβ4 from the cytokeratin fraction of ple (−/−) keratinocytes correlated well with the reduced number of HD-like structures found in these cells (Fig. 1, compare O with R; Andrä et al., 2003).

Collectively, these data supported the notion that the increased susceptibility of ple (−/−) keratinocytes to urea-induced deformation (as revealed by the conspicuous tangling of filaments and dramatic increase in the length of INTα6β4 retraction fibers), was caused by a lack of filament attachment to integrin clusters. On the other hand, the response of ple (+/+) and (−/−) cells to elevated temperatures in heat-shock assays was very similar, leading to a partial granulation of keratin filaments in both cases (unpublished data).

Plectin regulates IF disassembly dynamics

If, in the absence of plectin, the rigidity of IF networks is reduced and filaments are more loosely bound, or not bound at all, to the outer membrane, one might expect the network to be disassembled more readily in ple (−/−) compared with ple (+/+) cells. To test this, we monitored by immunofluorescence microscopy the kinetics of IF disassembly upon treatment of ple (+/+) and (−/−) cells with the serine/threonine phosphatase inhibitor okadaic acid (OA), which is known to selectively cause the disruption of IFs (Strnad et al., 2001). After a 2-h treatment of keratinocytes, the well-spread keratin network had formed thick bundles of filaments that seemed to be retracting toward the nucleus (Fig. 4 A, a and d, arrowheads). At later time points (4 and 6 h), a progressive breakdown of filaments was observed, with keratin granules forming first at the cell periphery (Fig. 4 A, e, arrowheads), followed by their collapse into a dense perinuclear ring (Fig. 4 A, e, arrow) that eventually became fragmented into numerous granules of various sizes (Fig. 4 A, f, arrow). The initial bundling of filaments appeared to occur more efficiently in ple (−/−) cells, as indicated by the increased mesh size of keratin networks visualized in the majority
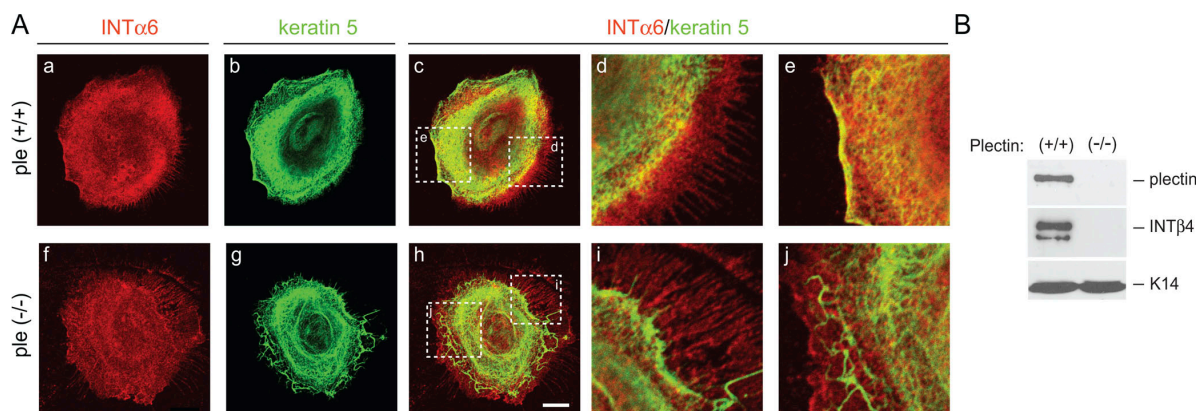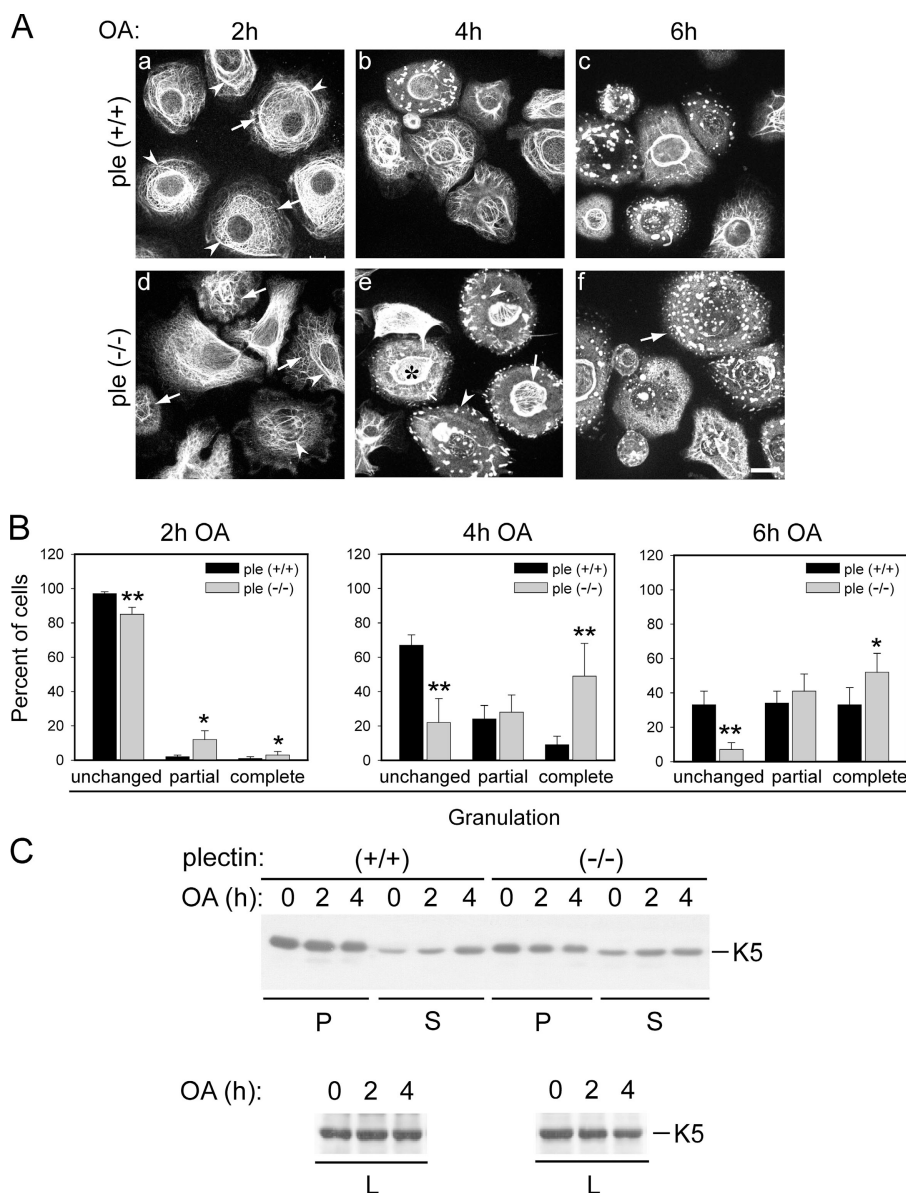
Figure 3. Keratin filaments of ple (−/−) keratinocytes are more sensitive to hypoosmotic shock and show reduced association with integrin α6/β4. (A) Osmotic shock–treated keratinocytes were fixed and immunolabeled for INTα6 and keratin 5. The boxed areas in c and h (designated with corresponding letters) are shown as ~3×-magnified images in d and e and i and j, respectively. Bar, 10 µm. (B) High-salt extracts from basal ple (+/+) and (−/−) keratinocytes grown on collagen I were subjected to immunoblotting using anti-plectin, -INTβ4 and –keratin 14 (K14) antibodies. Sample loadings were normalized to equal amounts of total protein.

of these cells compared with ple (+/+) cells (Fig. 4 A, a and d, arrows). Moreover, at the 4- and 6-h time points, the proportions of cells with keratin granules were significantly higher in ple (−/−) compared with ple (+/+) cells (Fig. 4 A, b and c and e and f). For a statistical analysis of keratin filament disassembly, cells were classified into three categories (1–3), where category 1 represented cells with no granules, category 2 represented cells with granules and residual filaments (Fig. 4 A, e, cell marked with asterisk), and category 3 represented cells in which complete granulation, including that of the perinuclear ring structure, had occurred (Fig. 4 A, f, cell marked with arrow). At the 2-h time point, ∼15% of ple (−/−) cells already fell into category 2, whereas only a mere 4% of ple (+/+) cells did (Fig. 4 B). After 4 h, the majority of the ple (−/−) cell population had their keratin network either partially (30%) or completely (50%) disassembled, whereas ∼70% of ple (+/+) cells were still without any granules (Fig. 4 B). After 6 h, the difference

between ple (+/+) and (−/−) cells became less pronounced, but ∼30% of ple (+/+) cells still did not show any granules, versus only ∼7% in the case of ple (−/−) cells (Fig. 4 B). Based on this, we concluded that the disassembly of IFs upon OA treatment is significantly accelerated in ple (−/−) compared with wild-type keratinocytes. In agreement with a previous study (Strnad et al., 2001), even after 6 h of OA treatment, no disruption of microtubules or microfilaments was observed. In fact, actin stress fiber formation was found to be significantly increased in ple (−/−) cells, and to some extent, also in ple (+/+) cells (unpublished data).

Plectin itself appeared to dissociate from IFs upon OA treatment of keratinocytes. Immunofluorescence microscopy revealed a strong increase in nonfilamentous (diffuse) plectin staining in keratinocytes at the 2-h time point (Fig. S3 A, available at http://www.jcb.org/cgi/content/full/jcb.200605172/DC1), whereas no colocalization with residual filaments nor with

Figure 4. **Faster OA-induced keratin filament disruption and soluble keratin pool elevation in plectin-deficient cells.** (A) Keratinocytes treated with OA for 2 (a and d), 4 (b and e), and 6 h (c and f) were immunolabeled using mAbs to pan-keratin. (a and d) Arrows, areas with increased keratin IF mesh size; (a and d) arrowheads, keratin filament bundling; (e) arrowheads, keratin granules; (e and f) arrows, examples of cells with perinuclear ring and completely fragmented ring, respectively. Bar, 20 μm. (B) Bar diagrams representing statistical evaluation of keratinocytes with complete, partial, and no (unchanged) filament breakdown. Cells marked with asterisk in A (e) and arrow in A (f) are representative examples of cells classified as showing partial and complete keratin granulation. Data shown represent mean values (± the SEM) of three different experiments (150 cells were counted from randomly chosen optical fields). * and **, P < 0.05 and P < 0.01, respectively. (C) Keratinocytes were either left untreated or treated with OA for the times indicated. Total cell lysates (L), detergent-soluble (S), and insoluble (P) cell fractions were subjected to immunoblotting using antibodies to K5 (similar results were obtained for K14).

keratin granules was observed at later time points (Strnad et al., 2001; unpublished data). Consistent with this, in cell fractionation experiments, plectin was no longer detectable in the cytokeratin fraction beyond the 2-h time point (Fig. S3 B).

Monitoring detergent-soluble keratin pools during OA treatment of keratinocytes, we found the level of soluble keratin proteins to already be elevated by approximately twofold in plectin-negative compared with wild-type cells before drug treatment (Fig. 4 C, 0 h). This difference further increased to approximately threefold within 2 h of drug treatment. Thereafter, keratin solubility in ple (−/−) cells stayed about level, while that in ple (+/+) cells further increased, approaching a level similar of that of ple (−/−) cells (Fig. 4 C, 4 h).

Plectin deficiency affects stress-activated p38 and Erk1/2 MAP kinases

Previous studies have shown stress-activated p38 MAP kinase to be one of the major candidates for mediating the effects of OA on vimentin and keratins (Cheng and Lai, 1998; Toivola et al., 2002). Therefore, we examined whether the OA-induced changes in network appearance and solubility of keratins were paralleled by changes in p38 activity. Using anti–phospho-p38 antibodies to monitor the activation status of p38 kinase, we found no significant differences between ple (+/+) and (−/−) keratinocytes under basal conditions (Fig. 5, A and B). Upon addition of OA to ple (−/−) cells, a moderate increase in p38 activity during the first hour was followed by a steep increase during the second hour and a sharp decline thereafter. In contrast, p38 kinase activity levels in ple (+/+) keratinocytes showed only a modest increase during the first 2 h, staying constant thereafter. Thus, the maximum of p38 activity measured in plectin-negative cells was more than twice as high as in wild-type cells.

To assess whether the elevated response of p38 kinase to OA in ple (−/−) cells was specific, the activity of another MAP kinase, Erk1/2, was monitored in a similar fashion. Unexpectedly,

we found the basal phosphorylation of Erk1/2 kinases to be already significantly elevated in ple (−/−) keratinocytes (Fig. 5, C and D) compared with ple (+/+) cells. Erk1/2 activities in ple (+/+) and (−/−) cells showed a similar response to OA treatment, however, reaching maxima after 1 h, followed by a decrease to levels below those observed before the treatment (Fig. 5, C and D). Hence, the accelerated OA-induced activation of p38 kinase in plectin-deficient, compared with wild-type, keratinocytes seemed to be specific for this MAP kinase, correlating with the observed tendency for faster keratin solubilization in these cells.

Faster in vitro migration of plectin-deficient compared with wild-type keratinocytes

Plectin-mediated attachment of the keratin cytoskeleton to INTα6β4 has been shown to play a crucial role in stabilizing adhesion of keratinocytes to the matrix, thereby inhibiting cell migration (Geuijen and Sonnenberg, 2002). Plectin-deficient keratinocytes, showing no association of INTα6β4 with keratins (Fig. 3 B), together with their up-regulation of Erk1/2 (see previous section), which is a kinase that positively regulates keratinocyte migration (Huang et al., 2004), prompted us to compare the migratory potentials of ple (+/+) and (−/−) keratinocytes using an in vitro wound-healing assay. Average migration distances measured for ple (−/−) cells were almost twice as long as those of ple (+/+) cells (Fig. 6, A and B). Interestingly, the mesh size of the keratin network in ple (−/−) keratinocytes along the wound edge was much larger compared with that of cells at a distance from the wound and, in these regions, differences to the keratin network of ple (+/+) cells became most prominent (Fig. 6 D, compare c with g). This was consistent with our finding that an increased keratin network mesh-size characteristic of ple (−/−) keratinocytes was particularly evident in subconfluent cell cultures (Fig. 1). Furthermore, in migrating wound-edge keratinocytes, plectin's

Figure 5. **Plectin deficiency is linked to accelerated OA-induced activation of p38 MAP kinase and alterations in Erk1/2 basal activity.** (A and C) Keratinocytes were either left untreated or treated with OA for the times indicated. Lysates from these cells were separated and immunoblotting was performed using antibodies to unphosphorylated/phosphorylated (total) or phosphorylated (P–) forms of p38 and Erk1/2, respectively. Tubulin, loading control. (B and D) Signal intensities of phosphorylated p38 and Erk2 bands, which were densitometrically determined in three independent experiments (including the one shown), were normalized to p38 and Erk2, respectively (mean ± the SEM). Curves represent OA-induced changes of corresponding values. au, arbitrary units. * and **, P < 0.05 and P < 0.01, respectively.
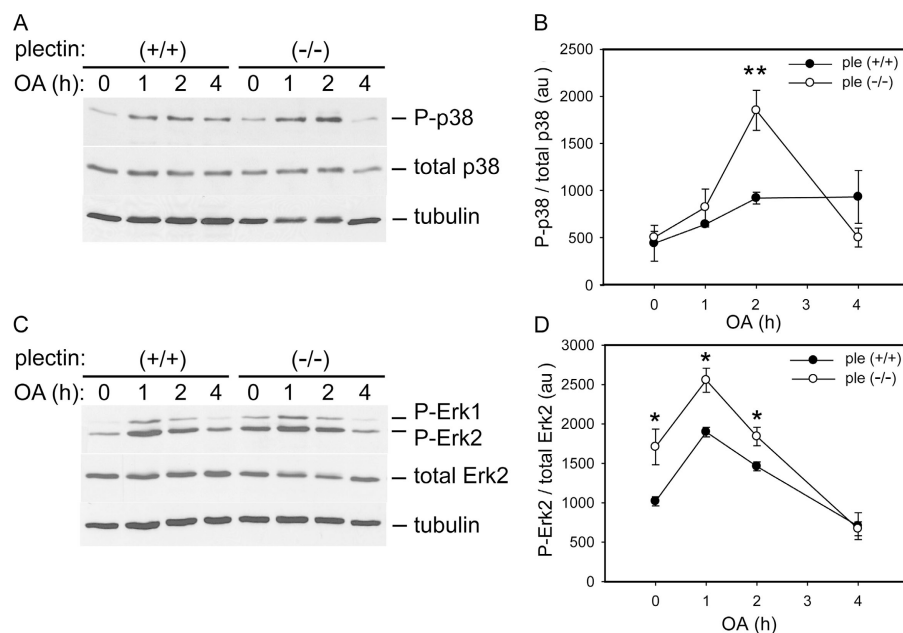
localization changed from basal integrin cluster– to keratin filament–associated (Fig. 6 D, compare a with e), highlighting the importance of plectin in organizing keratin cytoarchitecture during cell migration.

Because we had observed a correlation between the enhanced migration of ple (−/−) keratinocytes and the up-regulation of Erk1/2, we asked whether pharmacological inhibition of MEK1/2, which are the upstream kinases of Erk1/2, would decrease migration of ple (−/−) keratinocytes. As shown in Fig. 6, when ple (−/−) keratinocytes were exposed to PD98059, which is a specific inhibitor of MEK1/2 activities, their migration distances were reduced by almost a factor of two, bringing their level close to that of untreated wild-type cells. Wild-type cells showed a similar drug response. The observed decrease in

migration of drug-treated cells directly correlated with inhibition of Erk1/2 activities, as demonstrated by analysis of Erk1/2 phosphorylation (Fig. 6 C). A similar analysis showed that other MAP kinases, in particular JNK, were unaffected under these conditions (unpublished data).

Importantly, although MEK1/2 inhibition decreased the migration rate of ple (−/−) keratinocytes, it had no effect on their aberrant keratin network organization (Fig. 6 D, d and h), clearly placing plectin in the MAP kinase cascade upstream of Erk1/2. These data established a causal relationship between plectin deficiency and accelerated migration of keratinocytes, showing hyperactivation of Erk1/2 to be a consequence of plectin deficiency.

PKCδ and c-Src both have been suggested as major players in signaling pathways responsible for migration of keratinocytes
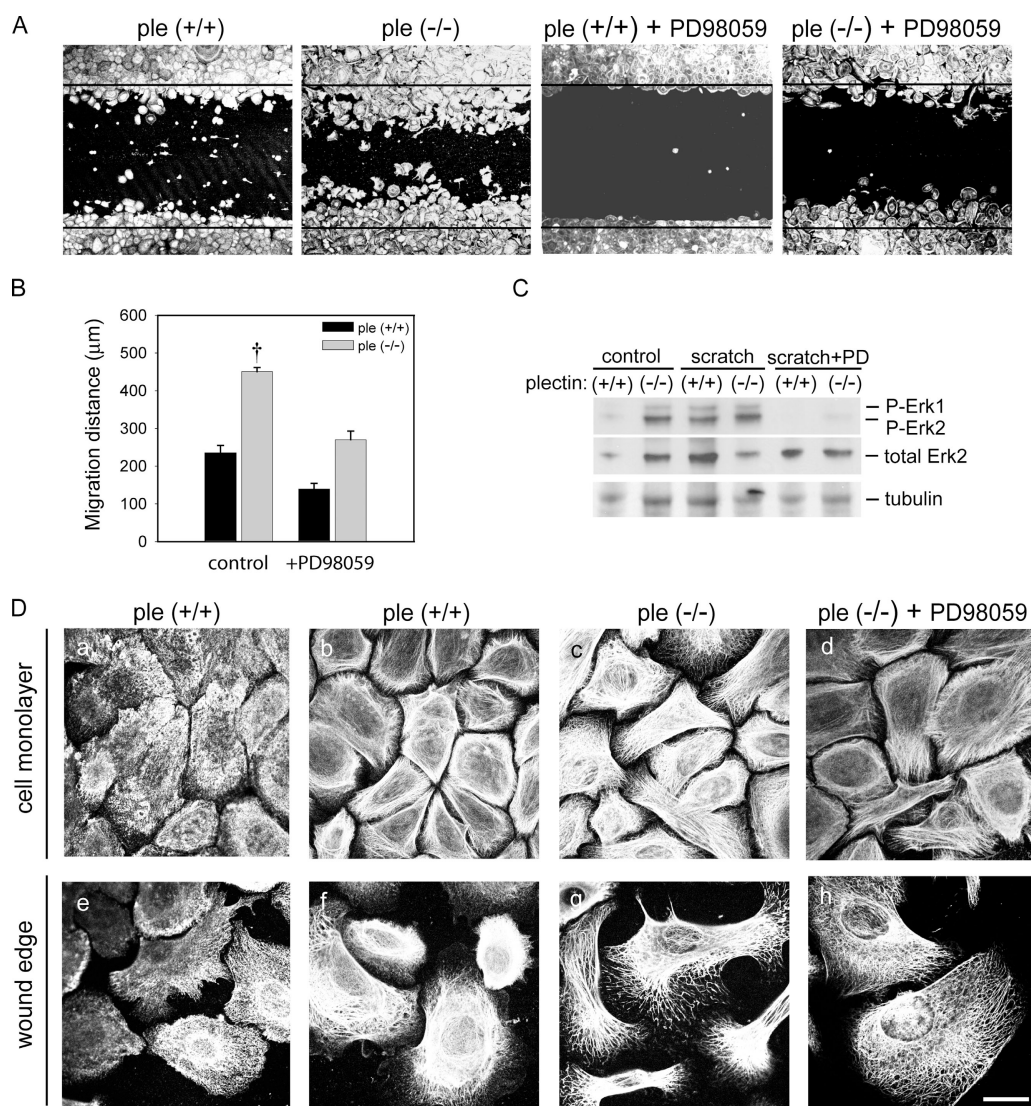
Figure 6. **Faster migration of ple (−/−) keratinocytes in scratch wound closure assays.** (A) Cells were stained using mAbs to actin (false gray color). The lines drawn in the images represent reference lines marking the width of the scratch when it was made. (B) Average values of migration distances from 10 different optical fields (10× objective) are shown (mean ± the SEM). †, $P < 0.001$. (C) Total cell lysates from controls, scratched cells (scratch) and PD98059-treated (PD) scratched cells were subjected to immunoblotting using antibodies to unphosphorylated/phosphorylated (total) Erk2, or phosphorylated (P–) Erk1/2. Tubulin was used as a loading control. (D) Representative images of keratinocytes in the interior of cell monolayers (a–d) and at the wound edge (e–h). (a and e) Antiserum to plectin; (b–d and f–h) mAbs to pan-keratin. Note increased keratin network mesh size of ple (−/−) cells at the wound edge. PD98058 had no effect on keratin filament cytoarchitecture (d and h). Bar, 10 μm.

(Yamada et al., 2000; Li et al., 2002), and both have been shown to be upstream activators of Erk1/2 (Miranti et al., 1999; Gagnoux-Palacios et al., 2003). Therefore, we next investigated activation of these kinases in membrane and cytosolic fractions of ple (+/+) and (−/−) keratinocytes. As shown in Fig. 7, A and B, both, PKCδ and c-Src kinase, exhibited increased phosphorylation (corresponding to higher activities) in the membrane fraction of ple (−/−) keratinocytes compared with wild-type cells. Although total c-Src levels in membrane and cytosolic fractions from both cell types were comparable, those of PKCδ were lower in the membrane fraction of ple (−/−) compared with ple (+/+) cells. In the cytosolic fractions, total PKCδ signals were hardly detectable in any of the two cell types.

To assess whether up-regulation of c-Src was related to enhanced Erk1/2-dependent migration of ple (−/−) keratinocytes, cells were treated with the Src family kinase inhibitor PP2, a suppressor of cell motility and Erk activation (Matsubayashi et al., 2004), before scratch wound assays. As expected, this treatment led to suppression of cell motility (unpublished data) and a dose-dependent decrease in phosphorylation (activity) of Erk1/2 (Fig. 7 C).

Forced expression of the plectin-binding protein RACK1 in keratinocytes leads to increased motility

In a previous study, we revealed a role of plectin as a cytoskeletal regulator of PKC signaling and possibly other signaling events (Osmanagic-Myers and Wiche, 2004). We proposed that plectin sequesters RACK1, which is a receptor and scaffolding protein of activated PKC and a direct binding partner of plectin, to the cytoskeleton when PKC is inactive. Because of the lack of its cytoskeletal docking site in the absence of plectin, in plectin-deficient cells RACK1 accumulates (together with PKC) at the periphery of cells, similar to the situation in wild-type cells after activation of PKC. According to this model, one may expect that the forced expression of RACK1 in wild-type kerat-

inocytes mimics the situation in ple (−/−) cells, leading to their characteristic phenotypes. To test this we analyzed the migration potential of keratinocytes expressing an EGFP-RACK1 fusion protein using time-lapse video microscopy.

In accordance with migration distances measured in scratch wound closure assays (Fig. 6), ple (−/−) keratinocytes displayed a migration velocity (1.58 μm/min) approximately two times as high as that of ple (+/+) cells (0.82 μm/min), when observed 2–6 h after plating (not depicted). As shown in Fig. 7 D (controls), 14–18 h after plating, ple (−/−) cells migrated three times as fast as ple (+/+) cells (1.53 vs. 0.49 μm/min). Expression of EGFP-RACK1 led to an increase in the average migration rates of both cell types. Transfected wild-type cells (1.30 μm/min) migrated 2.6 times faster than untransfected control cells, reaching 85% of the speed of untransfected ple (−/−) cells, whereas transfected ple (−/−) cells (2.02 μm/min) migrated 1.3 times faster than their untransfected counterparts. Similar experiments were performed with the cytoplasmic nonreceptor tyrosine kinase Fer, which, like RACK1, directly binds to plectin and thereby is inhibited in its activity (Lunter and Wiche, 2002). In this case the speed of wild-type cells was increased by approximately twofold (unpublished data).

In contrast, expression of an EGFP-plectin isoform 1a (full-length) fusion protein in ple (−/−) cells led to a significant slowdown of the cells, reducing their average speed to 0.98 μm/min (Fig. 7 D). This was equivalent to a slightly >50% rescue potential of the fusion protein, taking the values of control ple (+/+) and (−/−) cells into account. The lower rescue potential of plectin 1a in this assay compared with restoration of keratin network cytoarchitecture (Fig. 2 B) may reflect the requirement of other major isoforms expressed in keratinocytes, such as plectin 1c and 1 (Andrä et al., 2003), for full phenotype restoration. Thus, whereas overexpression of plectin-controlled signaling proteins, such as RACK1, led to downstream mechanisms boosting cell motility (Fig. 7), reexpression of a major

Figure 7. **Up-regulation of c-Src and PKCδ in ple (−/−) keratinocytes and increased migration potential of RACE1-overexpressing cells.** Measurement of various protein kinase activities (A–C) and time-lapse microscopy of migrating keratinocytes (D). (A and B) Membrane (Mem) and cytosolic (Cyt) subfractions of keratinocytes, normalized for equal protein contents, were immunoblotted using antibodies to unphosphorylated/phosphorylated (total) or phosphorylated (P–) c-Src and PKCδ. Caveolin and tubulin were used as loading controls. (C) Cell lysates from control cells and cells incubated with PP2, as indicated, were subjected to immunoblotting using antibodies to unphosphorylated/phosphorylated (total) Erk2 or phosphorylated (P–) Erk1/2. (D) ple (+/+) and (−/−) keratinocytes were transfected with EGFP-RACK1 (RACK1) or EGFP-plectin 1a (plectin) and monitored for migration over a period of 90 min. Untransfected cells served as controls. Values (mean ± the SEM) shown are based on the analyses of 20–30 cells per construct and genotype. * and **, P > 0.05 and P > 0.01, respectively.
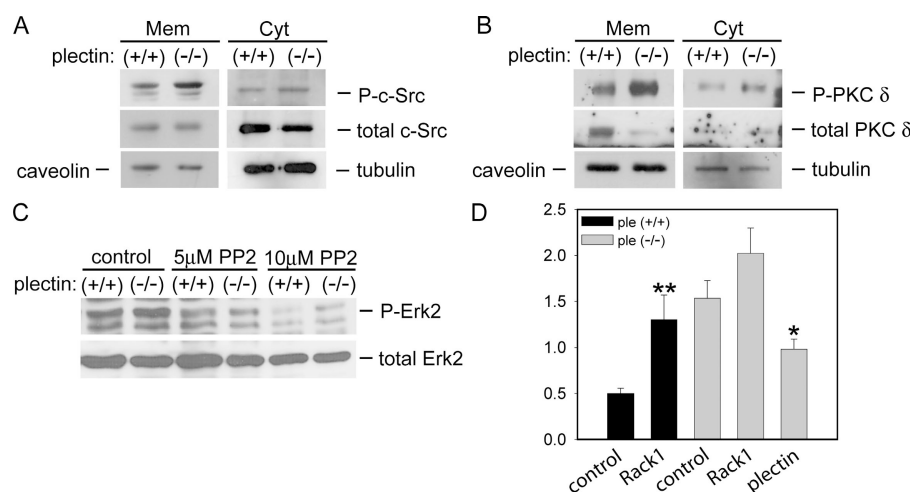
plectin isoform in ple (−/−) cells led to the partial reversal of their aberrant migration.

Discussion

Plectin organizes IF networks and contributes to cytoprotection against osmotic stress

This study provides evidence that plectin plays a crucial role in the appropriate organization of IF networks in keratinocytes. In plectin's absence, these networks are less delicate, their mesh size is increased, and individual filaments appear bundled and straighter. Plectin may control the properties of other IF systems as well, as alterations of IF networks resembling those described here for keratinocytes were also observed in plectin-deficient fibroblasts (unpublished data). Furthermore, a recent study suggests that plectin regulates both the organization and solubility of GFAP in astrocytes (Tian et al., 2006).

Based on ultrastructural analysis, we suggest that the mechanism behind the observed phenotype is a reduction of orthogonal cross-linkages between individual keratin IFs in the absence of plectin. In cross-linking individual filaments at high angles, plectin's interaction with IFs would resemble that of filamin with microfilaments. Such a mode of action would be consistent with earlier studies showing plectin to be predominantly localized at crossover and branching points of IFs (Foisner et al. 1988). Similar to filamin, plectin was shown to exist in dimeric and tetrameric states. Tetrameric structures are assumed to be formed by antiparallel alignment of two parallel plectin dimers (Wiche, 1998). Thus, exposed C-terminal IF-binding sites on both ends of such structure have the ability to cross-link two filaments. Even individual parallel dimers may have a cross-linking capacity, as an additional N-terminal vimentin-binding site resides in the N-terminal actin-binding domain of plectin (Sevcik et al., 2004). Oligomers of plectin tetramers, which are generated by the head-to-head fusion of dumbbell-shaped plectin molecules (Foisner and Wiche, 1987), have been shown to form at IF branching points (Foisner et al. 1988). Cross-linking functions of plectin have also been clearly demonstrated by Svitkina et al. (1996), who used immunogold electron microscopy to show that plectin is organized in millipede-like structures around the core of individual IFs, with plectin side-arms frequently making Y contacts with each other. Conceivably, such Y-shaped structures may emerge from head-to-head fusion of plectin molecules, allowing cross-linking at high angles. Moreover, these authors reported that plectin was not localized regularly all along IFs, but was more concentrated at their distal ends, which is consistent with our finding that defects in IF organization were most prominent in the peripheral regions of ple (−/−) cells.

The urea-based osmotic shock assay revealed a stronger stress response of ple (−/−) versus (+/+) keratinocytes, reflected by increased cell shrinkage and considerably longer retraction fibers. Suggesting an increased plasticity of ple (−/−) cells, these data also implied a role of plectin in stabilizing membrane surfaces. By interlinking IFs into properly organized three-dimensional networks, and by connecting these to the plasma membrane, plectin probably provides cell membranes with the required resistance against deformations, such as those induced by osmotic shock. A similar model has been proposed by Flanagan et al. (2001) to explain the increased deformability of filamin-deficient melanoma cells. Thus, plectin and filamin could have similar modes of action in respect to different cyto-skeletal filament systems.

What is the cause of accelerated IF network disassembly in ple (−/−) cells?

We assume that plectin increases the stiffness of IFs by introducing orthogonal cross-links between filaments and, thus, acts as a stabilizer opposing their disassembly. Moreover, the protein acts as a linker, anchoring keratin filaments to hemidesmosomal INTβ4, as shown on ultrastructural and biochemical levels (Fig. 4 B; Rezniczek et al., 1998). Further support for an IF-stabilizing role of plectin stems from differences in ple (+/+) and (−/−) keratinocytes during the early stages of OA-induced disassembly of IFs, which in wild-type cells correlates with the dissociation of plectin from keratin IF networks. The events after OA treatment can be viewed to parallel those of a more physiological process, i.e., mitosis, as in both cases plectin dissociates from IFs during their disassembly (Foisner et al., 1996). Thus, it seems that the release of stabilizing proteins such as plectin is a requirement for the efficient disassembly of IFs.

However, if the faster IF disassembly in ple (−/−) cells was strictly caused by the diminished mechanical stability of IFs, why did we observe a higher increase in p38 activity in these cells after OA-induced IF disassembly? It is unlikely that faster IF disassembly was caused by elevated levels of p38 kinase activity because, in this case, increased phosphorylation of keratins in ple (−/−) compared with wild-type cells should have been detected using p38 kinase site-specific phosphokeratin antibodies (Toivola et al., 2002). This, however, was not the case (unpublished data). Furthermore, there were no differences in the activity levels of p38 kinase between wild-type and ple (−/−) cells under basal conditions. Recently, an association of simple epithelial keratins 8/18 with Raf kinase and its disruption after treatment of cells with OA has been reported (Ku et al., 2004). Based on this, the authors suggested a role of keratins in sequestering a population of Raf and thereby regulating its signaling potential. In a similar fashion, keratins might regulate either p38 directly or one of its upstream effectors. Thus, we speculate that it is the faster disassembly of IFs and larger pool of their soluble subunits proteins in ple (−/−) compared with ple (+/+) cells that, via an unknown positive feedback mechanism, affects the activity of p38, rather than the other way around.

The plectin-ERK MAP kinase link and its consequences for keratinocyte migration

It is the currently accepted view that ligation of integrins triggers the activation of Erk, via either the adaptor protein Shc or some other mechanism (Wary et al., 1998). This has been shown to be the case for integrins of fibroblasts, as well as the integrin specific for keratinocytes, α6β4 (Mainiero et al., 1997). In some studies, the importance of integrin linkage to the cytoskeleton has been emphasized. For instance, in fibroblasts and skeletal
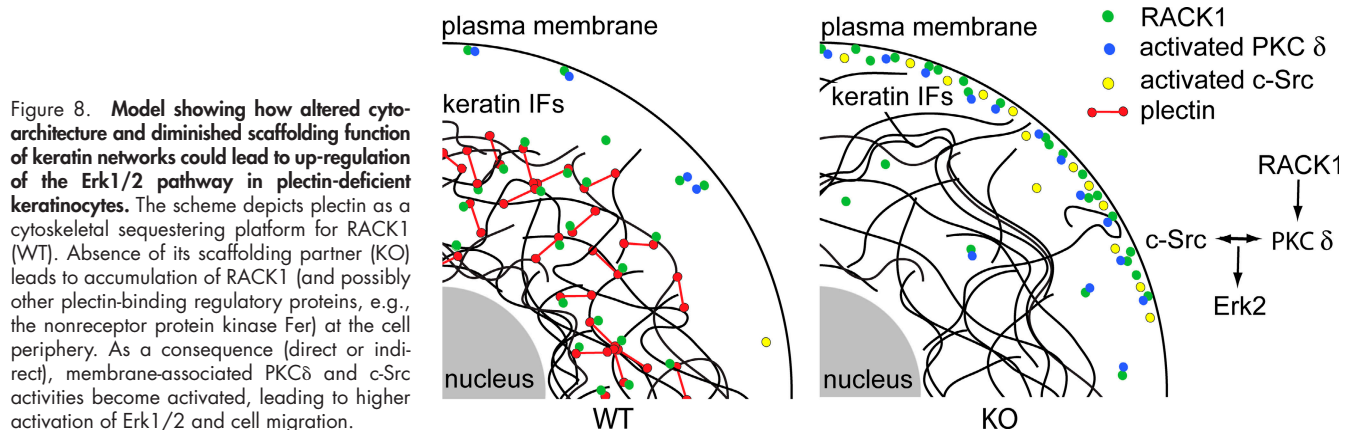
muscle cells, it was shown that the disruption of microfilaments with cytochalasin D blocked the integrin-mediated activation of MAP kinases (Zhu and Assoian, 1995). Similarly, a mutation in INTβ4 that prevents plectin–INTβ4 interaction leads to accelerated migration of keratinocytes (Geuijen and Sonnenberg, 2002). Fully in line with these studies, we demonstrate that plectin-deficient keratinocytes, showing no association of INTα6β4 with keratins, have an elevated migration potential. Most importantly, the migration of plectin-deficient cells was significantly reduced when plectin was reexpressed. An involvement in migration has recently been reported for another cytolinker family member, kakapo/short-stop (Fuss et al., 2004). By regulating Notch receptor localization and activity, short-stop was shown to be essential for the movement of proventricular cells during the invagination of foregut epithelium into endodermal midgut layers.

Our study shows that the increased migration potential of ple (−/−) compared with ple (+/+) keratinocytes is directly linked to elevated states of Erk kinase phosphorylation. Erk has been implicated in the migration of numerous cell types (Huang et al., 2004), and it has been shown to be the sole kinase responsible for ECM-initiated migration of keratinocytes (Li et al., 2004). On the other hand, enhancement and directionality of growth factor signaling is mediated by both Erk and p38 kinases, whereas JNKs were reported to be uninvolved in keratinocyte motility (Li et al., 2004). By pharmacological inhibition of Erk's upstream kinases MEK1/2, we were able to restore the aberrant high migratory potential of ple (−/−) keratinocytes to normal levels, but were unable to rescue the abnormal keratin network organization of these cells. Therefore, we feel it is safe to conclude that hyperactivation of Erk1/2 is a result of keratin network alterations caused by plectin deficiency, rather than the opposite. In support of this, keratinocytes from EBS patients, with mutations in keratins leading to spontaneous formation of keratin aggregates, migrate significantly faster in comparison to control cells (Morley et al., 2003). Although Erk activities were not investigated in this study, elevated basal levels of the stress-activated kinase SAPK/JNK found in these cells (D'Alessandro et al., 2002) were implicated in their faster migration. This raises the intriguing question of whether distinct alterations in keratin network organization, such as aggregation in keratin-

related EBS versus bundling in EBS caused by plectin deficiency, may lead to the up-regulation of distinct signaling pathways, such as SAPK/JNK versus MAPK. Studying human keratinocytes from an EBS-MD patient, Kurose et al. (2000) reported unaltered migration using phagokinetic track measurements. As these cells very likely expressed rodless isoforms of plectin, contrary to the plectin-null cells used in our study, it is difficult to compare both studies.

The signaling pathway leading from plectin-related keratin network alterations to hyperactivation of Erk1/2 still remains elusive. Our analysis conducted so far shows that the activities of two key proteins known to be involved in the regulation of keratinocyte migration, c-Src, and PKCδ are up-regulated in the membrane fraction of plectin-deficient cells, and that PP2-inhibition of c-Src indeed down-regulates Erk1/2 activities. Thus, membrane-associated c-Src and PKCδ are likely candidates for mediators of signals from plectin to Erk1/2. For the transduction of signals from the IF network to the membrane, our live-cell imaging data of transfected migrating keratinocytes, expressing EGFP-RACK1 fusion proteins, offer a plausible mechanistic explanation. Similar to a model proposed for PKCδ regulation through plectin-sequestration of RACK1 on IFs of fibroblasts (Osmanagic-Myers and Wiche, 2004), we propose that in keratinocytes regulatory (trigger) proteins of PKC, c-Src, and/or other upstream affectors of Erk1/2, are sequestered on IF-associated plectin molecules in a wild-type scenario, but are unbound to IFs and have free access to the membrane because of their missing anchor in plectin-deficient cells. The faster migration of cells overexpressing RACK1, which is shown in this study, is consistent with such a model. It will be of interest to characterize in more detail on the molecular level how c-Src and PKCδ become activated through signaling proteins such as RACK1 (and possibly Fer kinase) and what consequences this might have in different cell types. Fig. 8 A shows a scheme depicting the model proposed.

In conclusion, we believe the results reported have important implications for our understanding of the complexity involved in IF network regulation and formation and its influence on cell migration. In addition, they provide a better view on the actual severity and extent of EBS caused by plectin deficiency, as well as the basic molecular mechanism underlying this disease.

Figure 8. **Model showing how altered cyto-architecture and diminished scaffolding function of keratin networks could lead to up-regulation of the Erk1/2 pathway in plectin-deficient keratinocytes.** The scheme depicts plectin as a cytoskeletal sequestering platform for RACK1 (WT). Absence of its scaffolding partner (KO) leads to accumulation of RACK1 (and possibly other plectin-binding regulatory proteins, e.g., the nonreceptor protein kinase Fer) at the cell periphery. As a consequence (direct or indirect), membrane-associated PKCδ and c-Src activities become activated, leading to higher activation of Erk1/2 and cell migration.

Materials and methods

Cell culture, transient transfection, OA treatment, and osmotic shock assay

Primary keratinocytes were isolated from 1-d-old ple (+/+) and (−/−) mice according to the protocol described by Andrä et al. (2003). Cells were cultured on laminin 5–enriched matrices, which were prepared from 804G cell cultures (see below), and used for experiments without further passage of cells. Immortalized p53 (−/−) basal keratinocytes were derived from ple (+/+)/p53 (−/−) and ple (−/−)/p53 (−/−) mice (Andrä et al., 2003) cultured in KGM (Cambrex) on collagen I –coated (Sigma-Aldrich) plastic dishes. These cells were used at passage numbers 10–15, expressing keratins exclusively (Fig. S1). All initial key studies (IF phenotype and OA exposure experiments) were performed using primary keratinocytes and immortalized cell lines in parallel, with identical results. Because of the inability of primary keratinocytes to grow on collagen (Nguyen et al., 2001), all migration-related experiments (Figs. 6 and 7) were performed with immortalized cells. To obtain subconfluent cultures (used in all experiments except where indicated otherwise), cells were seeded at 8×10^3 cells/ml. Cells were exposed to 0.1 µg/ml OA (Sigma-Aldrich) for different time periods (for 1, 2, 4, and 6 h). For transient transfections we used Fugene reagent (Roche) according to the manufacturer's instructions. Expression plasmids encoded, tagged versions of full-length plectin isoform 1a (pGR245 and pVP37) or RACK1 (pSOS33). pGR245 and pVP37 were generated by subcloning plectin 1a cDNA into pEGFP-N2 (CLONTECH Laboratories, Inc.) or a modified pEGFP-N2 where EGFP was replaced by an Myc tag, respectively. pSOS33 was generated by subcloning RACK1 cDNA (provided by D. Mochly-Rosen [Stanford University, Stanford, CA] as plasmid pDM31) into pEGFP-C1 (CLONTECH Laboratories, Inc.). For preparation of laminin 5 matrices, rat bladder carcinoma 804G cells were cultured to confluence on plastic dishes in DME, washed once with PBS, and lysed with 20 mM NH_4OH for 5 min. Dishes were then washed thoroughly with water and kept in PBS (plus 10% DMSO) at −20°C. Osmotic shock stress assays were performed following the protocol of D'Alessandro et al. (2002).

Antibodies

For immunoblotting, the following primary and secondary antibodies were used: anti-K5 and -K6 antisera (PRB-160P and PRB-169P, respectively; Covance), mAbs LL001 to K14 (provided by J.M. Leigh, Royal London School of Medicine and Dentistry, London, England; Morley et al., 1995), mAbs LP34 (DakoCytomation) to K5, K6, and K18 (pan-keratin), a mixture of mAbs to K18 and K8 (Ks 18.04 and Ks 8.7, respectively; Progen), anti-plectin antiserum #9 (Andrä et al., 2003), anti-INTβ4 antiserum (provided by F.G. Giancotti, Memorial-Sloane Kettering Cancer Center, New York, NY; Mainiero et al., 1997), affinity-purified goat anti-vimentin antiserum (provided by P. Traub, University of Bonn, Bonn, Germany), mouse mAbs sc-535 to p38 (Santa Cruz Biotechnology, Inc.), rabbit mAbs 3D7 to phospho-Thr_{180}/Tyr_{182} p38 (Cell Signaling Technology), mAb D-2 to Erk2 (Santa Cruz Biotechnology, Inc.), mAbs E-4 to phospho-Tyr_{204} Erk1/2 (Santa Cruz Biotechnology, Inc.), anti–c-Src antiserum (Santa Cruz Biotechnology, Inc.), anti-phospho Y418 Src antiserum (Biozol), anti-phospho Thr_{505} PKCδ antiserum (Cell Signaling Technology), mAb P36520 to PKCδ (BD Biosciences), anti-caveolin antiserum (BD Biosciences), goat anti–rabbit IgG, goat anti–mouse IgG, and donkey anti–goat IgG (all from Jackson ImmunoResearch Laboratories), all conjugated to horseradish peroxidase. For immunofluorescence microscopy the following primary antibodies were used: anti-plectin antiserum #46 (Andrä et al., 2003), pan-keratin (see above), anti-K5 antiserum (see above), and rat mAbs to INTα6 (CD49f; BD Biosciences), mAbs B-5-1-2 to α-tubulin (Sigma-Aldrich), and affinity-purified antiserum and mAbs to actin (A 2066 and AC-40, respectively; Sigma-Aldrich). As secondary antibodies, we used goat anti–rabbit IgG Alexa Fluor 488 (Invitrogen), goat anti–rat IgG Texas red (Accurate Chemical & Scientific Corporation), goat anti–mouse IgG Texas red, donkey anti–mouse Rhodamine red-X, and donkey anti–goat Cy2 (all from Jackson ImmunoResearch Laboratories).

Immunofluorescence and electron microscopy

Cells grown overnight (∼12 h) were methanol-fixed, washed with PBS, mounted in Mowiol, and viewed in a laser-scanning microscope (LSM 510; Carl Zeiss MicroImaging, Inc.) at room temperature. Images were visualized with either a Plan-Apochromat 63×, 1.4 NA, or a Plan-Apochromat 100×, 1.4 NA, objective lens (Carl Zeiss MicroImaging, Inc.) using LSM software and processed using the Photoshop CS2 (Adobe) software package. For electron microscopy, cells grown on glass coverslips were washed three times with 0.15 M Sorensen`s buffer (SB), pH 7.4, before a 1-h fixation in

3% glutaraldehyde in SB. Cells were then washed twice with SB and post-fixed in 1% OsO4 in SB for 30 min. Subsequently, they were dehydrated in ethanol and flat-embedded in epoxy resin (Agar 100). Glass coverslips were removed from the Epon block by immersion in liquid nitrogen and subsequent warming. Thin sections (60–80 nm) were cut parallel to the plane of the cell layer, using an ultramicrotome (Leica). They were then mounted on copper grids, contrasted by uranyl acetate and lead citrate, and viewed at 60 kV in an electron microscope (JEM-1210; JEOL).

Preparation of cell fractions

After ∼12 h of adhesion, keratinocytes were washed twice with PBS and lysed directly with 50 mM Tris-HCl, pH 6.8, 100 mM DTT, 2% SDS, 1 mM Na_2VO_3, 1× phosphatase inhibitor cocktail 1 (Sigma-Aldrich), 1% bromo-phenol blue, and 10% glycerol (sample buffer). Aliquots of cell lysates containing equal amounts of total proteins were separated by SDS-PAGE and, after immunoblotting using peroxidase-coupled secondary antibodies, protein bands were visualized by exposure to x-ray film. Quantitation of bands was performed as previously described (Osmanagic-Myers and Wiche, 2004). Triton X-100 or high-salt extract fractions of keratinocytes were prepared according to Toivola et al. (2002). Membrane and cytosolic fractions were prepared according to a digitonin-based extraction protocol (Osmanagic-Myers and Wiche, 2004).

Scratch wound assay

ple (+/+)/p53 (−/−) and ple (−/−)/p53 (−/−) basal mouse keratinocytes were grown in parallel until reaching confluence (∼48 h). They were then treated with 10 µg/ml mitomycin C for 2 h. Subsequently, a scratch wound was introduced into the monolayer using a yellow Gilson pipette tip. Cells were washed three times with growth medium and further incubated for 24 h. For MEK1/2 or c-Src inhibition, 30 µM PD98059 (Cell Signaling Technology) or PP2 (Calbiochem), as indicated, were added to the growth medium 1 h before scratching and throughout the scratch closure period. Before fixation, a reference wound was inflicted to determine the original wound size. Cells were then fixed with methanol and processed for immunofluorescence microscopy using mAbs to actin, anti-plectin #46, and anti–pan-keratins. The average migration distance was calculated by subtracting the wound width after 24 h migration from that of the reference wound.

Live-cell imaging

Time-lapse video microscopy was implemented on a microscope (Axiovert S100TV; Carl Zeiss MicroImaging, Inc) equipped with phase-contrast and epiillumination optics. Cells were spread on collagen I–coated coverslips at a density of 2.8×10^5 cells/cm² and kept in KGM during the whole period of observation. Migration was monitored in a closed POCmini cultivation system (Carl Zeiss MicroImaging, Inc) at 37°C and 5% CO2. Recordings of migrations started 14 h after plating, and frames were taken with a 10× lens in 1-min intervals over a period of 90 min. Images were obtained using a back-illuminated, cooled charge-coupled device camera (Princeton Research Instruments) driven by a 16-bit controller. The whole video microscopy system was automated by Metamorph 6.3 (Universal Imaging Corporation). The length of trajectories of migrating cells was measured by tracking the central nuclei. Cells that did not spread or remain in the field of view during the whole period of observation were not taken into account for measuring. For statistical evaluation, we used 20–30 cells per construct and genotype.

Online supplemental material

Fig. S1 shows expression levels of keratins in wild-type and plectin-deficient cells monitored by immunoblotting. Fig. S2 shows that plectin and keratins colocalize with INTα6 at the cell periphery. Fig. S3 shows the dissociation of plectin from keratin filaments upon treatment of cells with OA. Online supplemental material is available at http://www.jcb.org/cgi/content/full/jcb.200605172/DC1.

References

Andrä, K., H. Lassmann, R. Bittner, S. Shorny, R. Fässler, F. Propst, and G. Wiche. 1997. Targeted inactivation of plectin reveals essential function

in maintaining the integrity of skin, muscle, and heart cytoarchitecture. *Genes Dev.* 11:3143–3156.

Andrä, K., B. Nikolic, M. Stöcher, D. Drenckhahn, and G. Wiche. 1998. Not just scaffolding: plectin regulates actin dynamics in cultured cells. *Genes Dev.* 12:3442–3451.

Andrä, K., I. Kornacker, A. Jörgl, M. Zörer, D. Spazierer, P. Fuchs, I. Fischer, and G. Wiche. 2003. Plectin-isoform-specific rescue of hemidesmosomal defects in plectin (−/−) keratinocytes. *J. Invest. Dermatol.* 120:189–197.

Cheng, T.J., and Y.K. Lai. 1998. Identification of mitogen-activated protein kinase-activated protein kinase-2 as a vimentin kinase activated by okadaic acid in 9L rat brain tumor cells. *J. Cell. Biochem.* 71:169–181.

D'Alessandro, M., D. Russell, S.M. Morley, A.M. Davies, and E.B. Lane. 2002. Keratin mutations of epidermolysis bullosa simplex alter the kinetics of stress response to osmotic shock. *J. Cell Sci.* 115:4341–4351.

Flanagan, L.A., J. Chou, H. Falet, R. Neujahr, J.H. Hartwig, and T.P. Stossel. 2001. Filamin A, the Arp2/3 complex, and the morphology and function of cortical actin filaments in human melanoma cells. *J. Cell Biol.* 155:511–517.

Foisner, R., and G. Wiche. 1987. Structure and hydrodynamic properties of plectin molecules. *J. Mol. Biol.* 198:515–531.

Foisner, R., F.E. Leichtfried, H. Herrmann, J.V. Small, D. Lawson, and G. Wiche. 1988. Cytoskeleton-associated plectin: in situ localization, in vitro reconstitution, and binding to immobilized intermediate filament proteins. *J. Cell Biol.* 106:723–733.

Foisner, R., N. Malecz, N. Dressel, C. Stadler, and G. Wiche. 1996. M-phase-specific phosphorylation and structural rearrangement of the cytoplasmic cross-linking protein plectin involve p34cdc2 kinase. *Mol. Biol. Cell.* 7:273–288.

Fuss, B., F. Josten, M. Feix, and M. Hoch. 2004. Cell movements controlled by the Notch signalling cascade during foregut development in *Drosophila*. *Development.* 131:1587–1595.

Gagnoux-Palacios, L., M. Dans, W. van't Hof, A. Mariotti, A. Pepe, G. Meneguzzi, M.D. Resh, and F. Giancotti. 2003. Compartmentalization of integrin α6β4 signaling in lipid rafts. *J. Cell Biol.* 162:1189–1196.

Geuijen, C.A., and A. Sonnenberg. 2002. Dynamics of the alpha6beta4 integrin in keratinocytes. *Mol. Biol. Cell.* 13:3845–3858.

Gregor, M., A. Zeöld, S. Oehler, K. Andrä-Marobela, P. Fuchs, G. Weigel, D.G. Hardie, and G. Wiche. 2006. Plectin scaffolds recruit energy-controlling AMP-activated protein kinase (AMPK) in differentiated myofibers. *J. Cell Sci.* 119:1864–1875.

Huang, C., K. Jacobson, and M.D. Schaller. 2004. MAP kinases and cell migration. *J. Cell Sci.* 117:4619–4628.

Ku, N.O., H. Fu, and M.B. Omary. 2004. Raf-1 activation disrupts its binding to keratins during cell stress. *J. Cell Biol.* 166:479–485.

Kurose, K., O. Mori, H. Hachisuka, H. Shimizu, K. Owaribe, and T. Hashimoto. 2000. Cultured keratinocytes from plectin/HD1-deficient epidermolysis bullosa simplex showed altered ability of adhesion to the matrix. *J. Dermatol. Sci.* 24:184–189.

Li, W., C. Nadelman, N.S. Gratch, W. Li, M. Chen, N. Kasahara, and D.T. Woodley. 2002. An important role for protein kinase C-delta in human keratinocyte migration on dermal collagen. *Exp. Cell Res.* 273:219–228.

Li, W., G. Henry, J. Fan, B. Bandyopadhyay, K. Pang, W. Garner, M. Chen, and D.T. Woodley. 2004. Signals that initiate, augment, and provide directionality for human keratinocyte motility. *J. Invest. Dermatol.* 123:622–633.

Lunter, P.C., and G. Wiche. 2002. Direct binding of plectin to Fer kinase and negative regulation of its catalytic activity. *Biochem. Biophys. Res. Commun.* 296:904–910.

Mainiero, F., C. Murgia, K.K. Wary, A.M. Curatola, A. Pepe, M. Blumemberg, J.K. Westwick, C.J. Der, and F.G. Giancotti. 1997. The coupling of alpha6beta4 integrin to Ras-MAP kinase pathways mediated by Shc controls keratinocyte proliferation. *EMBO J.* 16:2365–2375.

Matsubayashi, Y., M. Ebisuya, S. Honjoh, and E. Nishida. 2004. ERK activation propagates in epithelial cell sheets and regulates their migration during wound healing. *Curr. Biol.* 14:731–735.

McMillan, J.R., J.A. McGrath, M.J. Tidman, and R.A. Eady. 1998. Hemidesmosomes show abnormal association with the keratin filament network in junctional forms of epidermolysis bullosa. *J. Invest. Dermatol.* 110:132–137.

Miranti, C.K., S. Ohno, and J.S. Brugge. 1999. Protein kinase C regulates integrin-induced activation of the extracellular regulated kinase pathway upstream of shc. *J. Biol. Chem.* 274:10571–10581.

Morley, S.M., M. D'Alessandro, C. Sexton, E.L. Rugg, H. Navsaria, C.S. Shemanko, M. Huber, D. Hohl, A.I. Heagerty, I.M. Leigh, and E.B. Lane. 2003. Generation and characterization of epidermolysis bullosa simplex cell lines: scratch assays show faster migration with disruptive keratin mutations. *Br. J. Dermatol.* 149:46–58.

Morley, S.M., S.R. Dundas, J.L. James, T. Gupta, R.A. Brown, C.J. Sexton, H.A. Navsaria, I.M. Leigh, and E.B. Lane. 1995. Temperature sensitivity of the keratin cytoskeleton and delayed spreading of keratinocyte lines derived from EBS patients. *J. Cell Sci.* 108:3463–3471.

Osmanagic-Myers, S., and G. Wiche. 2004. Plectin-RACK1 (receptor for activated C kinase 1) scaffolding: a novel mechanism to regulate protein kinase C activity. *J. Biol. Chem.* 279:18701–18710.

Nguyen, B.P., X.-D. Ren, M.A. Schwartz, and W.G. Carter. 2001. Ligation of integrin α3β1 by laminin 5 at the wound edge activates rho-dependent adhesion of leading keratinocytes on collagen. *J. Biol. Chem.* 276:43860–43870.

Rezniczek, G.A., J.M. de Pereda, S. Reipert, and G. Wiche. 1998. Linking integrin α6β4-based cell adhesion to the intermediate filament cytoskeleton: direct interaction between the β4 subunit and plectin at multiple molecular sites. *J. Cell Biol.* 141:209–225.

Sevcik, J., L. Urbanikova, J. Kost'an, L. Janda, and G. Wiche. 2004. Actin-binding domain of mouse plectin. Crystal structure and binding to vimentin. *Eur. J. Biochem.* 271:1873–1884.

Steinböck, F.A., B. Nikolic, P.A. Coulombe, E. Fuchs, P. Traub, and G. Wiche. 2000. Dose-dependent linkage, assembly inhibition and disassembly of vimentin and cytokeratin 5/14 filaments through plectin's intermediate filament-binding domain. *J. Cell Sci.* 113:483–491.

Strnad, P., R. Windoffer, and R.E. Leube. 2001. In vivo detection of cytokeratin filament network breakdown in cells treated with the phosphatase inhibitor okadaic acid. *Cell Tissue Res.* 306:277–293.

Svitkina, T.M., A.B. Verkhovsky, and G.G. Borisy. 1996. Plectin sidearms mediate interaction of intermediate filaments with microtubules and other components of the cytoskeleton. *J. Cell Biol.* 135:991–1007.

Tian, R., M. Gregor, G. Wiche, and J.E. Goldman. 2006. Plectin regulates the organization of GFAP in Alexander Disease. *Am. J. Pathol.* 168:888–897.

Toivola, D.M., Q. Zhou, L.S. English, and M.B. Omary. 2002. Type II keratins are phosphorylated on a unique motif during stress and mitosis in tissues and cultured cells. *Mol. Biol. Cell.* 13:1857–1870.

Vasioukhin, V., C. Bauer, M. Yin, and E. Fuchs. 2000. Directed actin polymerization is the driving force for epithelial cell-cell adhesion. *Cell.* 100:209–219.

Wary, K.K., A. Mariotti, C. Zurzolo, and F.G. Giancotti. 1998. A requirement for caveolin-1 and associated kinase Fyn in integrin signaling and anchorage-dependent cell growth. *Cell.* 94:625–634.

Werner, N.S., R. Windoffer, P. Strnad, C. Grund, R.E. Leube, and T.M. Magin. 2004. Epidermolysis bullosa simplex-type mutations alter the dynamics of the keratin cytoskeleton and reveal a contribution of actin to the transport of keratin subunits. *Mol. Biol. Cell.* 15:990–1002.

Wiche, G. 1998. Role of plectin in cytoskeleton organization and dynamics. *J. Cell Sci.* 111:2477–2486.

Yamada, T., Y. Aoyama, M.K. Owada, H. Kawakatsu, and Y. Kitajima. 2000. Scraped-wounding causes activation and association of c-src tyrosine kinase with microtubules in cultured keratinocytes. *Cell Struct Funct.* 25:351–359.

Zhu, X., and R.K. Assoian. 1995. Integrin-dependent activation of MAP kinase: a link to shape-dependent cell proliferation. *Mol. Biol. Cell.* 6:273–282.